

Cation sensors containing a (bpy)Re(CO)₃ group linked to an azacrown ether *via* an alkenyl or alkynyl spacer: synthesis, characterisation, and complexation with metal cations in solution

Jared D. Lewis and John N. Moore*

Department of Chemistry, The University of York, Heslington, York, UK YO10 5DD

Received 23rd January 2004, Accepted 26th February 2004

First published as an Advance Article on the web 26th March 2004

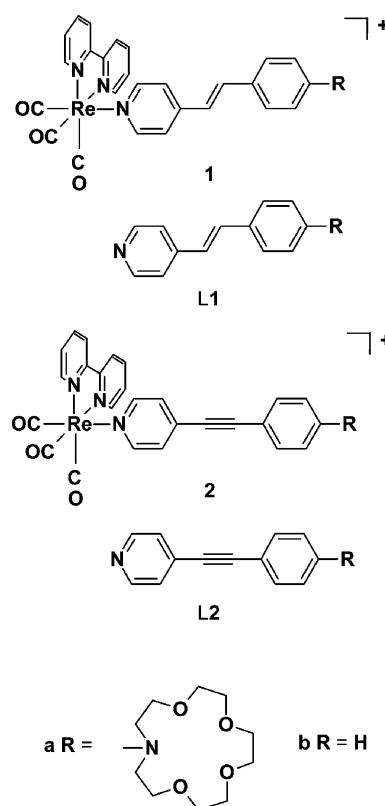
Two [(bpy)Re(CO)₃L]⁺ complexes (bpy = 2,2'-bipyridine), where L contains an aza-15-crown-5 ether which is linked to Re *via* an alkenyl- or alkynyl-pyridine spacer, have been synthesised along with model complexes. Solutions of the complexes in acetonitrile have been studied by UV-Vis absorption spectroscopy, and by 1D and 2D ¹H NMR spectroscopy. Strong UV-Vis bands, assigned to intraligand charge-transfer transitions localised at the L ligands, blue shift on protonation of the azacrown nitrogen atom or on complexation of alkali-metal (Li⁺, Na⁺ and K⁺) or alkaline-earth metal (Mg²⁺, Ca²⁺ and Ba²⁺) cations to the azacrown; the magnitude of the blue shift is dependent on the cation, with protonation giving the largest shift of *ca.* 100 nm. Cation binding constants in the range of log *K* = 1–4 depend strongly on the identity of the metal cation. Protonation or cation complexation causes downfield shifts in the ¹H NMR resonances from most of the azacrown and L ligand protons, and their magnitudes correlate with those of the blue shifts in the UV-Vis bands; shifts in the azacrown ¹H NMR resonances report on how the different metal cations interact with the macrocycle. UV-Vis and ¹H NMR spectra of the free L ligands enable the effect of the Re centre to be assessed. Together, the data indicate that the alkene spacer gives a more responsive sensor than the alkyne spacer by providing stronger electronic communication across the L ligand.

Introduction

There is considerable interest in molecules which bind cations in solution, and which incorporate functional groups that signal cation binding *via* the change in a molecular property that is easily detected.^{1,2} Such cation sensors have potential uses ranging from components in photonic communication devices to monitors of cation-dependent biological processes.^{3,4} Many reported systems contain crown ethers or their derivatives as receptors,⁵ with the binding of a cation inducing changes in the geometric or electronic structure of a signalling unit attached to the crown; such changes can usually be detected by conventional spectroscopy or by other simple physical techniques.

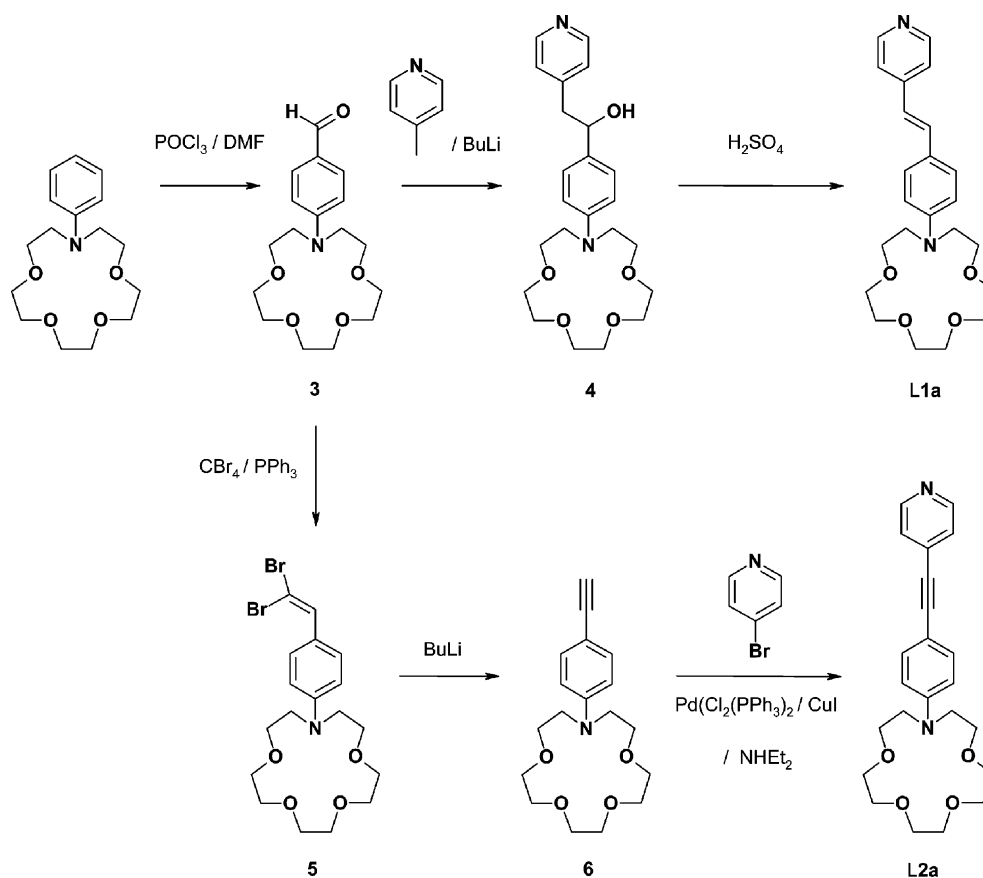
Azacrown ethers are common motifs in cation sensors because the azacrown nitrogen atom has a lone pair that can form part of a delocalised electron system, and so can provide very effective electronic communication between the receptor and the rest of the molecule, including the signalling unit. In many examples, the azacrown is attached to an organic dye and cation binding elicits a colour change that is easily monitored by UV-Vis spectroscopy.^{5–7} Our interest in such systems extends from sensors to “light-controlled ion switches” which are designed so that excitation of the chromophore results in cation ejection from the azacrown through effective electronic communication with the nitrogen atom which lowers the binding constant significantly on excitation.^{8,9}

In two recent communications, we presented two novel systems in which an azacrown ether is linked to a (bpy)Re(CO)₃ group *via* an alkenyl (**1a**)¹⁰ or alkynyl (**2a**)¹¹ spacer (Scheme 1), and we reported two notable photochemical properties: protonation of the azacrown regulates *trans–cis* photoisomerisation in the alkenyl system,¹⁰ and Ba²⁺ bound to the azacrown is ejected rapidly on excitation of the alkynyl system.¹¹ The rationale behind these molecular designs is that incorporating a transition-metal redox centre may bring additional excited-state decay routes and greater versatility in design than all-organic chromophore-azacrown systems. In particular, the (bpy)Re(CO)₃ group is being used increasingly in sensors because its metal-to-ligand charge-transfer (MLCT) excited state emits with a moderate quantum yield, and in photochemically active systems because it can undergo excited-state electron- and energy-transfer reactions.^{12–14} If the intention of incorporating



Scheme 1 Structures of complexes **1a**, **1b**, **2a** and **2b**.

a transition-metal centre is to mediate the binding properties of the azacrown, then clearly strong communication between these groups is required; consequently, complexes **1a** and **2a** have been designed with two different conjugated spacers in order to explore whether this may enhance their effectiveness as ion switches over other designs with weaker communication, such as those incorporating amide spacers.¹³ Moreover, designs with strong electronic communication across the molecule may also be expected to act as effective sensors, on the basis of our earlier work on azacrowns conjugated with organic dyes.^{7,15}



Scheme 2 Syntheses of L1a and L2a.

In this paper we focus on the ground states of **1a** and **2a**, and on their binding of metal cations. We report in full details of the synthesis and characterisation of these two azacrown complexes, their models **1b** and **2b**, and the respective L ligands without the Re group attached. We report UV-Vis and ^1H NMR studies of metal cation binding to the azacrown complexes **1a** and **2a**, including the measurement of binding constants. Parallel studies of the ligand **L1a** enable the effect of the Re centre within this generic design to be assessed, while a comparison of the results from **1a** and **2a** enables the effect of using alkene *versus* alkyne spacers to be considered. In addition to providing details of these systems as cation sensors, this work establishes a quantitative understanding of the ground-state spectroscopy and cation binding: this is an essential requirement prior to photochemical studies of ion switching.

Results and Discussion

Synthesis

The ligands **L1a** and **L2a** were prepared according to Scheme 2. The benzaldehyde **3** served as a common precursor to both of these ligands, and was prepared from the phenylaza-15-crown-5 *via* a Vilsmeier reaction.¹⁶ In the preparation of **L1a**, 4-methylpyridine was selectively deprotonated at the methyl group using LDA and reacted with **3** to produce the alcohol **4** which was dehydrated to generate **L1a**.¹⁷ In the preparation of **L2a**, **3** was converted first to the alkene **5** *via* a Wittig reaction with the ylide reagent generated from mixing PPh_3 with CBr_4 under anhydrous conditions (Corey–Fuchs method).¹⁸ This dibromo-vinyl derivative **5** was reacted with BuLi to generate a lithium acetylide¹⁹ which afforded **6** on aqueous work-up; **6** was coupled to the 4-position of a pyridine ring through a Sonogashira–Hagihara cross-coupling reaction²⁰ to generate **L2a**. The models were prepared in an identical manner to the respective azacrown analogues except that benzaldehyde was used in place of **3** to prepare **L1b**, and ethynylbenzene was used

in place of **6** to prepare **L2b**. All of the Re complexes were prepared by a procedure reported for different L ligands:^{13,21} $(\text{bpy})\text{Re}(\text{CO})_3\text{Cl}$ was prepared initially and then $\text{CF}_3\text{SO}_3\text{H}$ was used to produce $(\text{bpy})\text{Re}(\text{CO})_3(\text{CF}_3\text{SO}_3)$, which was reacted with <1 equivalent of the appropriate L ligand to generate its Re complex.

Characterisation

The UV-Vis spectra of the **1a**, **1b**, **2a** and **2b** complexes, and the **L1a** and **L1b** ligands, all in acetonitrile, are shown in Fig. 1. Both of the **1a** and **2a** complexes give intense visible absorption bands, at 428 and 404 nm, respectively, and a comparison of the **1a** and **L1a** spectra shows that they arise from transitions localised on the respective L ligand: they are assigned to intra-ligand charge-transfer (ILCT) transitions, in which charge is transferred from the azacrown nitrogen donor to the ethenylpyridyl or ethynylpyridyl acceptor.¹³ The model complexes **1b** and **2b** give similar bands, at *ca.* 330 and 310 nm, respectively, which are also assigned to transitions localised on the respective L ligand: the shift to higher energy and the decrease in absorption strength may be attributed to a loss of charge-transfer character due to the absence of an azacrown electron donor in these ligands. All of the complexes also show weaker bands at <320 nm which can be assigned to $\pi \rightarrow \pi^*$ transitions localised on bipyridine and L ligand groups. The Re \rightarrow bpy MLCT absorption bands of the complexes, which occur at *ca.* 350 nm in related complexes and typically have peak absorption coefficients of $\epsilon_{\text{max}} \approx 4000 \text{ mol}^{-1} \text{ dm}^3 \text{ cm}^{-1}$,^{14,22} underlie the strong L-centred bands, which have $\epsilon_{\text{max}} \approx 40000\text{--}50000 \text{ mol}^{-1} \text{ dm}^3 \text{ cm}^{-1}$.

The 500 MHz ^1H NMR spectrum of **1a** in CD_3CN is shown in Fig. 2, and assignments according to the numbering in Scheme 3 are given in Table 1 along with those for the model complex **1b** and the ligand **L1a**. The spectra of **2a** and **2b** are similar to those of **1a** and **1b**, and the same numbering scheme is used; H12 and H13 are absent in the alkynes.

The spectrum of **1a** is assigned as follows. The group of resonances at *ca.* δ 3.5, with a combined integration of 20H, is readily assigned to protons on the azacrown ether ring, with individual protons assigned according to the literature.¹⁵ The

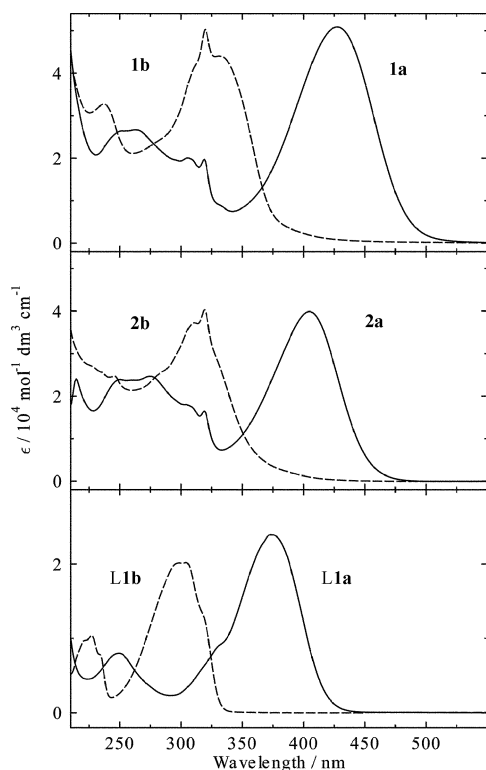
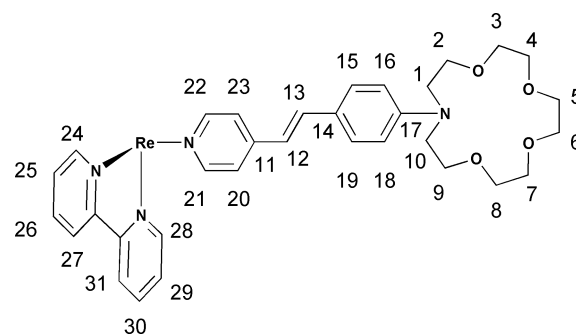


Fig. 1 UV-Vis absorption spectra of complexes **1a**, **1b**, **2a** and **2b**, and the ligands **L1a** and **L1b**, in acetonitrile.



Scheme 3 Numbering scheme for assignment of ^1H NMR resonances of **1a**; an identical numbering scheme was used for **2a**, with H12 and H13 absent.

other resonances are assigned according to the expected pattern, in which the bipyridyl group gives two doublets and two triplets, in the range δ 7.5–9.3 reported for 2,2'-bpy,²³ the pyridyl and aryl groups of L each give a characteristic AA'BB' pattern of two doublets, and the alkene group gives two doublets. ^1H - ^1H COSY and NOESY spectra were used to assign the resonances of **1a** to each of these fragments. COSY cross-peaks between the triplets at δ 8.26 and 7.79 and the doublets at δ 8.37 and 9.22, respectively, indicated that these four resonances could be assigned to the bpy ligand. A NOESY cross-peak between the bpy resonance at δ 9.21 and the doublet at δ 8.01 allowed these resonances to be assigned to H(24,29) on bpy and to H(21,22) on the pyridyl ring of L, respectively. The remainder of the bpy resonances and the other pyridyl resonance were then assigned using the COSY cross-peaks. Two NOESY cross-peaks were also present between the azacrown resonances at δ 3.53–3.68 and a doublet at δ 6.70 which was therefore assigned to H(16,18) on the aryl ring of L, enabling

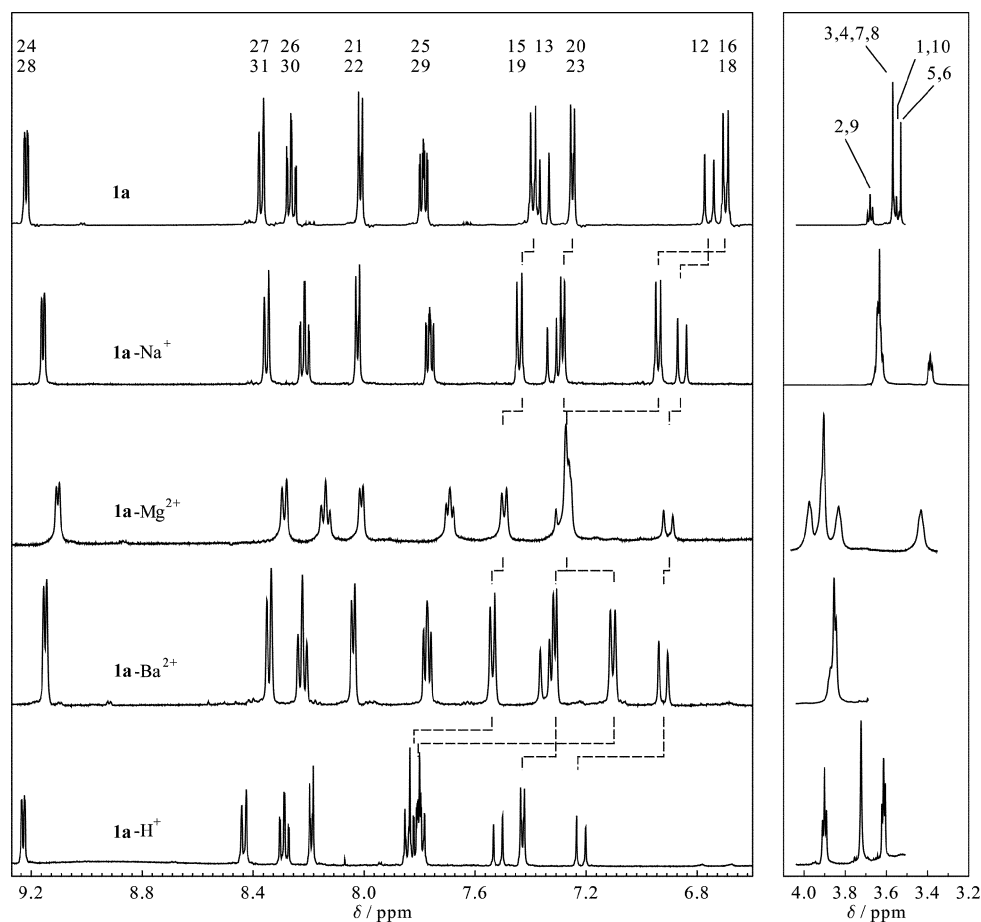


Fig. 2 500 MHz ^1H NMR spectra of **1a** and of **1a** with selected cation salts added in large excess, all in CD_3CN . Dashed lines show shifts in the resonances of H(15,19) H(20,23), H(12), and H(16,18).

Table 1 Chemical shifts, δ (in ppm) from the 500 MHz ^1H NMR spectra of **1a**, **1b**, **L1a**, **2a** and **2b** in CD_3CN , along with the shifts in the resonances, $\Delta\delta = \delta_{\text{bound}} - \delta_{\text{free}}$, on complexation of **1a** and **2a** with cations; numbering given in Scheme 3

Compound	H(5,6)	H(1,10)	H(3,4,7,8)	H(2,9)	H(16,18)	H(12)	H(20,23)	H(13)	H(15,19)	H(25,29)	H(21,22)	H(26,30)	H(27,31)	H(24,28)
δ														
1b	—	—	—	—	7.40	7.08	7.40	7.47	7.59	7.81	8.14	8.28	8.39	9.24
L1a	3.56	3.57	3.60	3.71	6.73	6.89	7.40	7.35	7.44	—	8.47	—	—	—
1a	3.53	3.55	3.57	3.68	6.70	6.76	7.25	7.35	7.39	7.79	8.01	8.26	8.37	9.22
$\Delta\delta$														
1a–Li⁺	0.08	0.06	0.04	0.08	0.14	0.07	0.04	0.00	0.05	–0.01	0.03	–0.01	0.01	0.02
1a–Na⁺	0.02	–0.23	–0.02	–0.13	0.25	0.10	0.03	–0.02	0.04	–0.01	0.03	–0.04	–0.01	–0.05
1a–Mg²⁺	0.22	–0.27	0.18	0.04	0.57	0.29	0.14	–0.07	0.11	–0.12	0.00	–0.14	–0.10	–0.13
1a–Ca²⁺	–0.24	0.23	0.21	0.10	0.48	0.14	0.02	–0.06	0.10	–0.08	–0.02	–0.10	–0.08	–0.11
1a–Ba²⁺	0.17	0.15	0.13	0.02	0.40	0.16	0.06	–0.02	0.15	–0.03	0.02	–0.05	–0.04	–0.09
1a–H⁺	0.07	0.05	0.13	0.21	1.11	0.47	0.19	0.17	0.42	0.06	0.19	0.04	0.07	0.02
δ														
2b	—	—	—	—	7.45	—	7.35	—	7.56	7.81	8.22	8.28	8.39	9.22
2a	3.53	3.55	3.57	3.68	6.69	—	7.25	—	7.33	7.79	8.12	8.27	8.38	9.21
$\Delta\delta$														
2a–Li⁺	0.12	0.10	0.05	0.10	0.13	—	–0.02	—	0.04	–0.01	0.02	–0.02	0.01	–0.03
2a–Na⁺	0.03	–0.20	–0.01	–0.10	0.21	—	–0.01	—	0.03	–0.04	–0.01	–0.06	–0.04	–0.07
2a–Mg²⁺	0.23	–0.26	0.18	0.07	0.50	—	0.03	—	0.10	–0.14	–0.02	–0.16	–0.11	–0.15
2a–Ca²⁺	–0.24	0.23	0.21	0.10	0.50	—	–0.04	—	0.11	–0.08	–0.02	–0.11	–0.09	–0.12
2a–Ba²⁺	0.22	0.20	0.18	0.07	0.40	—	0.01	—	0.13	–0.05	–0.01	–0.07	–0.06	–0.10

the final doublet at δ 7.25 to be assigned to H(20,23) on the pyridyl ring of L. The two doublets at δ 6.76 and 7.35, with integrations of 1H, were assigned to the vinyl protons; the large coupling constants of *ca.* 17 Hz for these doublets indicate that **1a** was prepared exclusively as the *trans*-isomer. One NOESY cross-peak between the pyridyl resonance at δ 7.25 and the vinyl resonance at δ 7.35 enabled it to be assigned to H(13) due to its close proximity to H(23); and another cross-peak between the aryl resonance at δ 7.39 and the other vinyl resonance at δ 6.76 enabled it to be assigned to H(12) due to its similarly close proximity to H(19).

The resonances in the spectrum of **2a** were assigned in an identical manner to those of **1a**, and those of **1b**, **L1a**, and **2b** were assigned readily using the assignments for **1a** and **2a**. There is a significant downfield shift in the resonances of the L ligands on going from **1a** and **2a** to **1b** and **2b**, respectively, with shifts of *ca.* 0.7 ppm for H(16,18) and *ca.* 0.2 ppm for H(15,19) on the aryl rings, and *ca.* 0.1 ppm for H(20,23) and H(21,22) on the pyridyl rings; the resonances from the vinyl protons of **1** also show downfield shifts of 0.32 ppm for H(12) and 0.12 ppm for H(13). These shifts indicate that the L ligand protons are more deshielded in **1b** and **2b** due to the absence of the electron-donating N-atom of the azacrown; the magnitude of the shift correlates broadly with the distance of the proton from the azacrown. By contrast, the resonances from the bpy protons show very small downfield shifts of 0.01–0.02 ppm, indicating that these protons are essentially unaffected by the absence of the azacrown.

Protonation and cation complexation

The UV-Vis spectra of **1a** and **2a** in acetonitrile show a blue shift in the ILCT absorption band as NaClO_4 is added (Fig. 3): no further changes were observed above a salt concentration of *ca.* 0.14 mol dm^{-3} , and the presence of isosbestic points indicates that an equilibrium between two species is observed. Similar blue shifts in ILCT absorption bands have been observed on cation binding to the azacrown in related complexes,^{5,7} and therefore the spectra indicate the formation of **1a–Na⁺** and **2a–Na⁺**, respectively, according to the general case in eqn. (1).

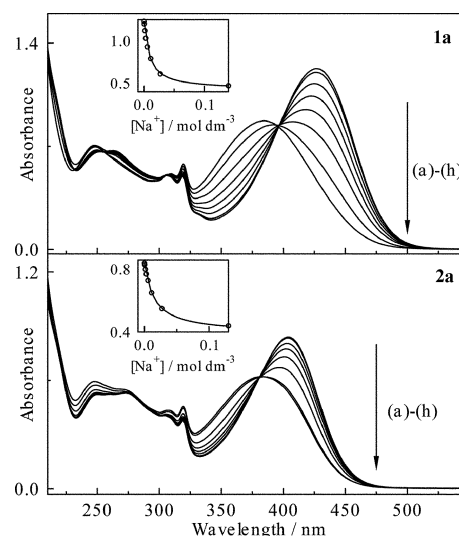


Fig. 3 UV-Vis absorption spectra of **1a** (*ca.* 2.5×10^{-5} mol dm^{-3}) and **2a** (*ca.* 2.1×10^{-5} mol dm^{-3}) in acetonitrile containing tetrabutylammonium perchlorate at 0.1 mol dm^{-3} to maintain constant ionic strength, and at 23 °C, with NaClO_4 at (a) 0, (b) 2.7×10^{-4} , (c) 1.4×10^{-3} , (d) 2.7×10^{-3} , (e) 5.4×10^{-3} , (f) 1.1×10^{-2} , (g) 2.7×10^{-2} and (h) 0.14 mol dm^{-3} . Insets: absorbance versus NaClO_4 concentration for **1a** at 428 nm and for **2a** at 404 nm; the solid lines are the best fits to eqn. (2).

Similar changes to those observed on addition of NaClO_4 were observed on addition of other alkali or alkaline-earth metal salts or HCl to **1a** and **2a**. The spectra obtained under limiting conditions of high salt concentrations are shown in Fig. 4, along with those for **L1a** (discussed below).

The largest blue shift of the ILCT band is caused by protonation (Table 2), and the spectra of **1a–H⁺** and **2a–H⁺** (Fig. 4) are notably similar to those of **1b** and **2b** (Fig. 1). These spectra indicate that H^+ binds exclusively to the azacrown N-atom,²⁵ and that the electron-donor properties of the azacrown nitrogen atom are effectively removed in both cases. The magnitude of the blue shift is smaller for all of the other cations, and it varies with cation identity (Fig. 4; Table 2). The shift is larger for the di-cations than the mono-cations, and Fig. 5 shows that it correlates broadly with the charge density of the cation.²⁶ Thus, the small and doubly charged Ca^{2+} elicits a larger shift than the larger Ba^{2+} , and both cause larger shifts

Table 2 Absorption maxima, λ_{max} (in nm), of **1a**, **2a** and **L1a** in acetonitrile, and blue shifts, $\Delta\lambda$ (in nm) on cation complexation, along with cation radii for six-coordination, r (in Å),²⁴ and charge-to-radius ratios, (z/r) (in Å⁻¹)

Cation	r	z/r	1a		2a		L1a	
			λ_{max}	$\Delta\lambda$	λ_{max}	$\Delta\lambda$	λ_{max}	$\Delta\lambda$
none	—	—	428	—	404	—	374	—
Li ⁺	0.76	1.32	402	26	386	18	361	13
Na ⁺	1.02	0.98	385	43	376	28	342	32
K ⁺	1.38	0.72	404	24	390	14	355	19
Mg ²⁺	0.72	2.78	342	86	327	77	324	50
Ca ²⁺	1.00	2.00	351	77	341	63	319	55
Ba ²⁺	1.49	1.34	362	66	350	54	329	45
H ⁺	—	—	319	109	307	97	—	—

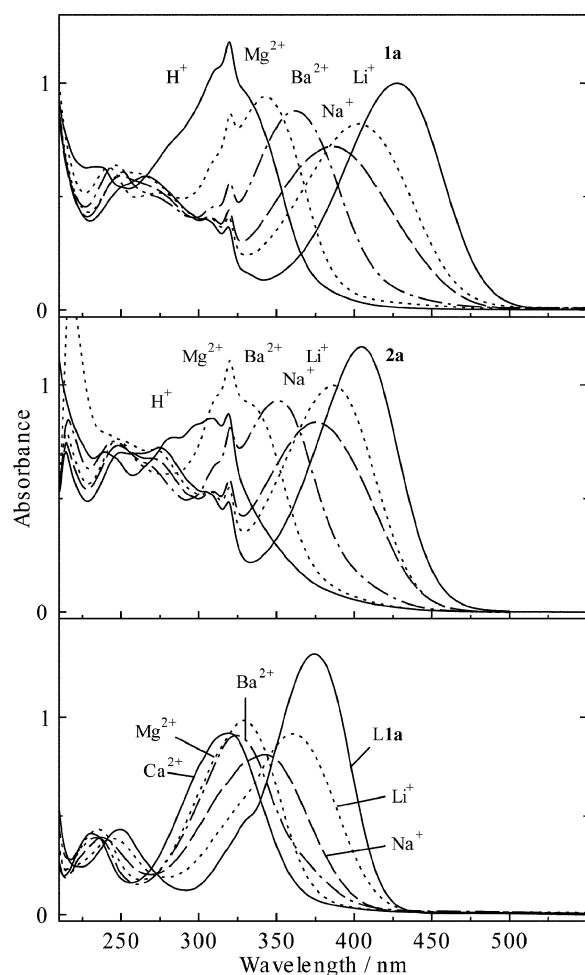


Fig. 4 UV-Vis absorption spectra of **1a**, **2a**, and **L1a** in acetonitrile, and in the presence of selected cations (ca. 0.14 mol dm⁻³) approaching saturation of the spectral changes.

than singly charged Na⁺ and K⁺, which are of similar respective size. Li⁺ gives a shift which is smaller than that predicted by the general trend, consistent with this hard cation binding preferentially to the oxygen atoms and interacting only weakly with the nitrogen atom, as discussed in the literature.^{7,25,27,28} Mg²⁺ is similar in size to Li⁺ but, by contrast, it gives the largest shift apart from H⁺, indicating that Mg²⁺ interacts strongly with the azacrown N-atom. The trend in bandshift *versus* cation is similar for **1a** and **2a**, consistent with the presence of the same azacrown in both complexes.

The ¹H NMR spectra of **1a** and **2a** in CD₃CN show shifts in the resonances on addition of alkali and alkaline-earth metal salts, and on addition of HCl.²⁹ Sample spectra are shown in Fig. 2 for **1a** samples at limiting salt concentrations which UV-Vis spectra confirmed were of fully complexed forms.^{30,31}

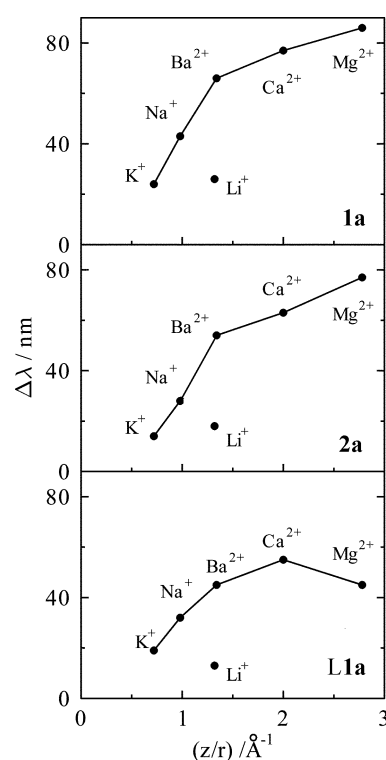


Fig. 5 The hypsochromic shift on complexation ($\Delta\lambda$) *versus* the cation charge-to-radius ratio (z/r) for **1a**, **2a** and **L1a**; solid lines illustrate the general trend.

Shifts in resonances on cation binding ($\Delta\delta = \delta_{\text{bound}} - \delta_{\text{free}}$) are given for **1a** and **2a** in Table 1, and identified by dashed lines in Fig. 2 for the H(16,18), H(15,19), H(12), and H(20,23) resonances of **1a**. In each case, the largest shift on binding is a downfield shift in the resonance of H(16,18), located on the aryl ring of L and nearest to the azacrown. There are also relatively large downfield shifts in the resonances of the other aryl ring protons H(15,19), and both up- and downfield shifts in the resonances of various azacrown protons H(1–10) depending on the identity of the bound cation. For **1a**, there are relatively large downfield shifts in the resonance of the vinyl proton H(12), and generally small upshifts in that of the other vinyl proton H(13). Shifts in the resonances of protons on the pyridyl ring of L, and on the bpy ligand, are generally small. These observations are consistent with cation binding at the azacrown, and with the ¹H NMR assignments made above for **1a** and **2a**.

The downfield shifts in the H(16,18) and H(15,19) resonances of **1a** and **2a** may be attributed to deshielding of the aryl protons due to the electrostatic effect of the cation bound to the adjacent azacrown; similarly large shifts in the aryl ring ¹H resonances on cation binding have been reported for organic azacrown-containing molecules with similar structures.^{15,27} The magnitude of the shift in the aryl ring and vinyl proton resonances *versus* cation identity shows a trend which is broadly consistent with that of the magnitude of the ILCT band shifts in the UV-Vis spectra of **1a** and **2a**: H⁺ elicits the largest downfield shift in H(16,18) and H(12), followed by Mg²⁺, Ca²⁺ and Ba²⁺; Na⁺ and Li⁺ cause significantly smaller shifts, with the small effect of Li⁺ being consistent with it binding preferentially to the azacrown oxygen atoms. This trend is consistent with H⁺ and Mg²⁺ causing the greatest disruption to the electronic structure of the L ligand *via* a strong interaction with the azacrown nitrogen atom.

The various up- and downfield shifts in the resonances of the azacrown protons H(1–10) may be attributed to both the location of the bound cation and to the changes it induces in the conformation of the azacrown ring, both of which may be expected to depend strongly on the identity of the cation. The

Table 3 Binding constants ($\log K$) for complexation of metal cations with **1a** and **2a** in acetonitrile, along with ranges reported for various related aza-15-crown-5-ether dyes in acetonitrile^{6,7,27,33,34}

Cation	$\log K$		
	1a	2a	N-15-C-5 dyes
Li ⁺	2.63 ± 0.03	2.44 ± 0.06	1.7–2.8
Na ⁺	2.05 ± 0.03	1.82 ± 0.03	1.4–2.2
K ⁺	1.40 ± 0.15	1.04 ± 0.04	1.3–2.2
Mg ²⁺	2.98 ± 0.07	2.76 ± 0.06	1.6–2.7
Ca ²⁺	4.30 ± 0.11	3.32 ± 0.08	1.7–4.2
Ba ²⁺	3.16 ± 0.24	2.80 ± 0.06	1.9–3.6

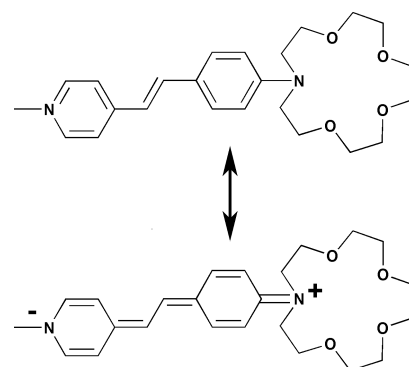
pattern of the azacrown ring resonances reports on the location of the cation. In the absence of a bound cation, the resonances divide into four sets, indicating that four magnetic environments exist: H(1,10) adjacent to the N-atom; H(2,9) next removed; H(3,4,7,8) in the centre; and H(5,6) furthest from the N-atom (Fig. 2; Table 1). On binding H⁺, Li⁺, or Mg²⁺, which are small cations that locate in specific parts of the ring, a shifted but similar pattern to that in the absence of the cation is maintained, with three (H⁺) or four (Li⁺, Mg²⁺) distinct resonances indicating that the ring retains three or four different environments. On binding Ba²⁺, which is a large cation that is expected to locate above the centre of the ring, a quite different pattern is obtained with all of the resonances occurring at a similar chemical shift (Fig. 2), indicating that all of the protons experience a similar environment. Na⁺ and Ca²⁺, which are of similar and intermediate size, both give an intermediate pattern of two distinct resonances.

Cation binding constants

For 1:1 complexation according to eqn. (1), binding constants K can be calculated from spectrophotometric titrations using eqn. (2), and where: A_0 , A , and A_∞ are the absorbances at a fixed wavelength in the absence of M^{n+} , in the presence of M^{n+} , and in the limiting case of infinite cation concentration, respectively; and the total ligand and total metal concentrations are $[L]_{\text{tot}} = [L] + [LM^{n+}]$ and $[M^{n+}]_{\text{tot}} = [M^{n+}] + [LM^{n+}]$, respectively.³²

The insets within Fig. 3 illustrate non-linear regression analyses using eqn. (2), with A_0 fixed at the value in the absence of added NaClO₄ and the limiting value of A_∞ fitted as one of the parameters. The data fit well to eqn. (2), substantiating the validity of applying eqn. (1) and providing binding constants of $K = 112 \pm 8$ and $66 \pm 5 \text{ dm}^3 \text{ mol}^{-1}$ for Na⁺ with **1a** and **2a**, respectively. All of the cation binding constants obtained by this method are given in Table 3.

The binding constants obtained for **1a** and **2a** are comparable to those reported both for an analogous complex in which aza-15-crown-5 is linked to (bpy)Re(CO)₃ by an amide spacer,¹³ and for other systems in which aza-15-crown-5 is linked to a dye (Table 3),^{6,7,27,33,34} but they are smaller than those for aza-15-crown-5 itself (*e.g.*, $\log K = 5.68$ for Na⁺).³⁵ This effect has been attributed to a decrease in the electron density on the azacrown nitrogen atom arising from its interaction with an attached chromophore in dye systems, as illustrated by the resonance structures shown in Scheme 4,⁷ and it may be stronger in the Re complexes **1a** and **2a**, which carry a positive charge. To assist in rationalising the magnitudes of the binding constants, we have performed DFT calculations on **ML1a** and **ML2a** (Fig. 6), which serve as models for **L1a** and **L2a**, respectively, using diethylamino groups in place of azacrowns to simplify the calculation. This approach has



Scheme 4 Resonance structures of **L1a**.

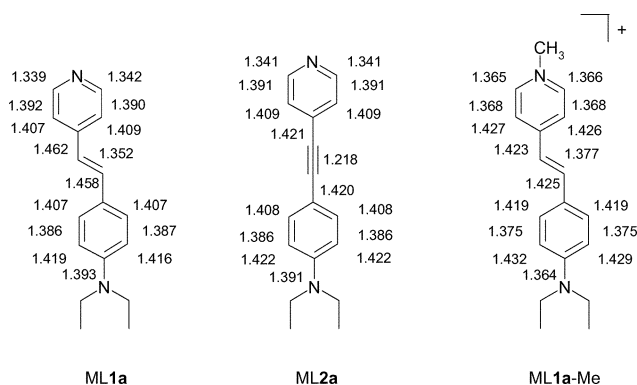


Fig. 6 Structures calculated by DFT for **ML1a**, **ML2a**, and **ML1a-Me**, which model **L1a**, **L2a**, and **1a**, respectively (see text); selected bond lengths given in Å.

been adopted successfully in reported semiempirical and DFT calculations.^{36–38}

The calculated structures of **ML1a** and **ML2a** show that the ligands are remarkably planar between the two nitrogen atoms, which is consistent with observed X-ray crystallographic structures of similar systems¹⁵ and indicates that there is strong conjugation throughout the pyridyl and aryl ring systems and the alkenyl or alkynyl spacers.⁷ Selected bond lengths given in Fig. 6 show that the aryl and pyridyl rings are both partially quinoidal, which is consistent with a strong contribution to the ground-state electronic structure from the charge-separated resonance form shown in Scheme 4. In both **ML1a** and **ML2a**, the short bond length between the aryl ring and the azacrown N-atom (*ca.* 1.392 Å), in particular, indicates that there is strong interaction between the nitrogen lone pair and the aryl ring π -electrons. Fig. 6 also shows the results of a DFT calculation on **ML1a-Me**, in which **ML1a** has been methylated at the pyridyl nitrogen atom to create a positively charged species to model the effect of coordination to a positively charged Re atom, as in **1a**. The bond lengths, and particularly the shorter bond between the aryl ring and the azacrown N-atom (1.364 Å), are consistent with an increased contribution from the charge-separated form on attaching an electron-acceptor at the pyridyl group. Thus, the DFT calculations on these models provide further support for the interpretation of the relatively low binding constants of **1a** and **2a** represented by Scheme 4.

The variation in the magnitude of the cation binding constants with cation identity (Table 3) do not correlate with those of the cation-induced bandshifts (Table 2), as also reported for other azacrown sensors.^{7,36,39} However, the variation in binding constant with cation identity observed here for both **1a** and **2a** is similar to that reported for other systems in which aza-15-crown-5 is linked to a dye (Table 3): it has been rationalised

$$A = A_0 + \frac{(A_\infty - A_0)}{2[L]_{\text{tot}}} \left([L]_{\text{tot}} + [M^{n+}]_{\text{tot}} + \frac{I}{K} - \sqrt{\left([L]_{\text{tot}} + [M^{n+}]_{\text{tot}} + \frac{I}{K} \right)^2 - 4[L]_{\text{tot}}[M^{n+}]_{\text{tot}}} \right) \quad (2)$$

through a combination of effects, including size-matching between azacrown and cation, the thermodynamics of cation desolvation required for azacrown complexation, and the nature of the interaction between these hard cations and the hard oxygen and soft nitrogen atoms of the macrocycle.⁴⁰ Ca²⁺, in particular, binds strongly to the azacrown: its diameter of 2.00 Å is well-matched to the aza-15-crown-5 cavity diameter of 1.7–2.2 Å. Na⁺ has a similar diameter of 2.04 Å but a much smaller binding constant: the higher charge density of Ca²⁺ may mean that the enthalpy change on binding with the azacrown and/or the gain in entropy associated with desolvation are more favourable.

Effect of the Re centre on sensor properties

The changes in the UV-Vis and NMR spectra of **1a** and **2a** on cation complexation arise principally from changes that are localised at the L ligand; the free ligands **L1a** and **L2a** themselves can act as cation sensors in the absence of the Re centre. A comparison of the UV-Vis and ¹H NMR spectra of the free ligand **L1a** with those of the Re complex **1a** enables the effect of the Re centre to be assessed.

The UV-Vis spectra of **L1a** obtained on addition of salts at limiting concentrations are shown in Fig. 4. The ILCT band of **L1a** ($\lambda_{\text{max}} = 374 \text{ nm}$; $\epsilon_{\text{max}} = 24\,000 \text{ dm}^3 \text{ mol}^{-1} \text{ cm}^{-1}$) is at shorter wavelength and is weaker than that of **1a** ($\lambda_{\text{max}} = 428 \text{ nm}$; $\epsilon_{\text{max}} = 51\,000 \text{ dm}^3 \text{ mol}^{-1} \text{ cm}^{-1}$), and the magnitude of the blue shift on cation binding is smaller for **L1a** than for **1a** (Table 2). The observation that **1a** is a more responsive UV-Vis sensor than **L1a** may be attributed to the increased charge polarisation that results from coordinating the positively charged Re centre, as indicated by the DFT calculations discussed above. The ILCT absorption bands of similar donor-acceptor ligands have also been observed to red shift on coordination to metal centres, with the magnitude of the shift dependent on the charge of the metal centre and on ancillary ligands.^{41,42} Therefore, the increased responsiveness in UV-Vis cation sensing reported here on coordination of **L1a** to Re is likely to be a general effect which could be enhanced by coordination to metal centres which are stronger acceptors than the (bpy)Re(CO)₃ group, e.g. to highly charged metal centres with strong π -acid ligands. However, an increase in the UV-Vis spectral response due to increased charge polarisation may be accompanied by a decrease in binding constants, and hence in a decrease in sensitivity to cation concentration, as discussed above.

The largest changes in the ¹H NMR spectra on going from **L1a** to **1a** are upfield shifts of 0.46 and 0.15 ppm in the resonances of H(21,22) and H(20,23), respectively, on the pyridyl ring (Table 1). The resonance of the vinyl proton H(12) also shifts upfield, by 0.13 ppm, whereas that of the other vinyl proton H(13) does not shift. The aryl proton resonances show small upfield shifts of 0.05 and 0.03 ppm for H(15,19) and H(16,18), respectively. These shifts indicate that the L ligand protons are more shielded in **1a** than **L1a**, and that the magnitude of the effect correlates broadly with the distance of the proton from the Re centre. These observations are consistent with the interpretation that coordination to the Re centre increases the electron demand at the pyridyl ring of the L ligand and enhances the charge-transfer character of the ground state (Scheme 4).

Alkene versus alkyne spacers

The ILCT bands of **1a** and **L1a** are at longer wavelength and are more intense than those of **2a** and **L2a**, respectively (Fig. 1), indicating that the charge-transfer state is at lower energy and that there is a larger transition dipole moment for **1a** and **L1a** than for **2a** and **L2a**. Hence, the electronic communication between the azacrown electron-donor and the pyridyl electron-acceptor in these systems is stronger *via* an alkene than an alkyne spacer. This is consistent with the general literature on

alkene *versus* alkyne spacer systems,⁴³ which attributes the difference to comparatively poor sp²–sp π -overlap in aryl–alkyne systems, arising from a mismatch in the respective p-orbital energies;⁴⁴ the DFT calculations suggest that the systems studied here are both approximately planar and, hence, that twisting of the aryl rings due to steric effects⁴⁵ is unlikely to be significant in either system. The trend in the magnitude of the ILCT band shift with cation identity is the same for **1a** and **2a** (Table 2, Fig. 5), and the larger shifts for **1a** than **2a** may be attributed to stronger electronic communication in the alkene system. The differences in the UV-Vis spectra of **1a** and **2a** provide useful information on the relative strength of electronic communication, but they are relatively small; Figs. 4 and 5 show that both complexes can act effectively as sensors.

The ¹H NMR spectra of **1a** and **2a** are closely similar. The largest differences on going from **1a** to **2a** are a downfield shift of 0.11 ppm in the resonance of H(21,22) on the pyridyl ring and an upfield shift of 0.06 ppm H(15,19) on the aryl ring. These shifts are consistent with the interpretation that the ground state of **1a** has greater charge-transfer character than that of **2a** due to stronger electronic communication. The shifts in the ¹H NMR resonances with cation identity are broadly similar for **1a** and **2a**.

The cation binding constants of **1a** and **2a** are within an order of magnitude of each other, but the values for **1a** are consistently higher than those for **2a** (Table 3: typically, log *K* ca. +0.3 higher; *K* ca. $\times 2$ higher). This is the converse of what would be expected if the relative magnitudes of the binding constants were determined simply by the extent of charge-transfer in the ground state (Scheme 4), which is greater for **1a** than **2a**. However, the cation binding constants of a large range of alkene-linked aza-15-crown-5-dyes have been shown not to correlate with the charge on the azacrown N-atom but, instead, to correlate with the charge on the complete NR₂ functionality, including the alkyl groups.³⁶ This correlation indicates that the binding constant is determined not only by the charge at the azacrown N-atom but also by the charges on the alkyl groups resulting from hyperconjugation, *i.e.* R→N electron donation *via* σ – π mixing that increases with increasing pyramidalization at the nitrogen atom.

The structures of the models calculated by DFT (Fig. 6) show that **ML1a** is partly pyramidal whereas **ML2a** is essentially planar, as quantified by the sums of the bond angles around the azacrown nitrogen atom: the calculated values are 356.1° and 359.9°, corresponding to differences from planarity of 3.9° and 0.1° for **ML1a** and **ML2a**, respectively. Moreover, although the calculated negative charge on the N-atom itself (Q_{N}) is lower for **ML1a** than **ML2a**, consistent with Scheme 4, the calculated positive charge on the whole diethylamino group (Q_{DEA}) is lower for **ML1a** than **ML2a**, consistent with increased σ – π mixing due to greater pyramidalisation:³⁶ the calculated values are $Q_{\text{N}} = -0.493$ and -0.503 , and $Q_{\text{DEA}} = +0.364$ and $+0.384$ for **ML1a** and **ML2a**, respectively. Thus, the calculations on **ML1a** and **ML2a** suggest that the higher binding constants of **1a** than **2a** can be rationalised in terms of partial pyramidalisation at the azacrown N-atom in the alkene system resulting in an increased partial positive charge on the whole azacrown.

Conclusions

These studies establish a quantitative understanding of the UV-Vis and ¹H NMR spectra of the azacrown-containing [(bpy)Re(CO)₃L]⁺ complexes **1a** and **2a**, and of their protonation and complexation of alkali and alkaline-earth metal cations. Strong ILCT bands enable these systems to act as responsive UV-Vis sensors to cations. A stronger spectral response than the free L ligand is obtained by attaching the Re group, which causes an increase in the charge-transfer character of the system; and a stronger spectral response by **1a** than **2a** is attributed to

stronger electronic communication *via* an alkene rather than an alkyne spacer. The ^1H NMR spectra of **1a** and **2a** show shifts in the resonances on cation binding which provide complementary information on structure, with the pattern of azacrown resonances reporting on the location of the cation within the ring. The lower cation binding constants of **1a** and **2a** than aza-15-crown-5 ether itself are attributed to the charge-transfer character of these systems, while stronger binding constants for **1a** than **2a** can be rationalised by the electronic effects of partial pyramidalisation at the azacrown N-atom in **1a**. Our interest in **1a** and **2a** extends to their possible application as light-controlled cation switches, and our studies of their photochemistry will be reported elsewhere.

Experimental

Spectroscopic and computational methods

UV-Vis spectra were recorded with a Hitachi U-3010 spectrometer, using chromophore concentrations in the range $(1.6\text{--}2.5) \times 10^{-5}$ mol dm $^{-3}$ and at 23 °C. Solutions of **2a** with added cation perchlorate salt were prepared in the dark in order to avoid any photoisomerisation.¹⁰ Anhydrous acetonitrile was used to determine binding constants, and tetrabutylammonium perchlorate at 0.1 mol dm $^{-3}$ was used to maintain constant ionic strength. UV-Vis spectra were processed using Grams 386 software (Galactic Industries Corp.), and binding constants were obtained by nonlinear regression analyses performed using SPSS software (SPSS Inc.) with uncertainties quoted as 95% confidence limits. 270 MHz ^1H NMR spectra were recorded to characterise the synthesis products using a JEOL EX spectrometer, with CDCl $_3$ as solvent and referenced against the protiated solvent signal at 7.24 ppm. 500 MHz 1D and 2D ^1H NMR spectra were recorded for more detailed studies using a Bruker AMX 500 spectrometer, with CD $_3$ CN as solvent and referenced against the protiated solvent signal at 1.96 ppm. NMR data were recorded at a temperature of 300 K and at chromophore concentrations of *ca.* 1×10^{-3} mol dm $^{-3}$. Electrospray ionisation mass spectra (ESI-MS) were recorded on a Finnigan LCQ instrument: typical isotope patterns were observed, and the values quoted here correspond to the more abundant ^{187}Re isotope. Elemental analyses were performed by Elemental Microanalysis Ltd. Density functional theory (DFT) calculations were performed using Gaussian 98 software:⁴⁶ all calculations used the B3LYP functional and the 6-31G(d) basis set.

Materials

Lithium perchlorate, sodium perchlorate, potassium thiocyanate, hydrochloric acid, trifluoromethanesulfonic acid, diethylamine, diisopropylamine, 4-methylpyridine, BuLi (1.6 mol dm $^{-3}$ in hexanes), zinc dust, PPh $_3$, NH $_4$ Cl, CBr $_4$, 4-bromopyridine hydrochloride, 4-ethynylbenzene, copper(I) iodide, dichlorobis(triphenylphosphine)palladium(II), 2,2'-bipyridyl, POCl $_3$ and NH $_4$ PF $_6$ (all Aldrich) were used as received. Magnesium perchlorate, barium perchlorate, calcium perchlorate (all Aldrich) were dried under vacuum at 230 °C and stored under nitrogen before use; tetrabutylammonium perchlorate (Aldrich) was dried similarly but at 60 °C. MgSO $_4$ and NaOH were obtained from Fisher, 1-phenyl-(4,7,10,13-tetraoxa-1-azacyclopentadecane) (phenylaza-15-crown-5) from Acros Organics and VWR International, P $_2$ O $_5$ from Avocado, and Re(CO) $_5$ Cl from Strem: all were used as received. General solvents for synthetic work were obtained from Fisher; anhydrous acetonitrile, THF, and CH $_2$ Cl $_2$ were obtained from Aldrich; CDCl $_3$ was obtained from Cambridge Isotope Laboratories and CD $_3$ CN from Aldrich. Silica gel for column chromatography (silica gel 60, 35–70 mesh) was obtained from Fluorochem and TLC plates (silica gel 60, F $_{254}$) from Merck.

Syntheses

L ligands

4-(4,7,10,13-Tetraoxa-1-azacyclopentadecyl)benzaldehyde (3). This was prepared by following a reported procedure.¹⁶ Pale green crystals were obtained. Yield 72%; ^1H NMR (270 MHz, CDCl $_3$) δ 3.6–3.8 (m, aliphatic crown) 6.67 (d, 2H, *J* 9.2 Hz, aromatic), 7.68 (d, 2H, *J* 9.2 Hz, aromatic), 9.70 (s, 1H, CHO).

1-[4-(4,7,10,13-Tetraoxa-1-azacyclopentadecan-1-yl)phenyl]-2]pyridin-4-ylethanol (4). This was prepared by following a reported procedure for an NEt $_2$ derivative.¹⁷ Diisopropylamine (651 mg, 6.4 mmol) was dissolved into 2 cm 3 of dry THF under N $_2$. BuLi solution (4 cm 3 , 6.4 mmol) in 5 cm 3 THF was added under N $_2$ at 0 °C and stirred for 0.5 h. 4-Methylpyridine (600 mg, 6.4 mmol) was added at –78 °C and the solution turned deep red. After stirring for 90 min, **3** (1.98 g, 6.4 mmol) in 10 cm 3 THF was added dropwise and the now light-red solution was stirred for 5 h. H $_2$ O (30 cm 3) was then added and the solution turned yellow. The mixture was extracted $\times 3$ into Et $_2$ O and the organic layer retained and dried over MgSO $_4$. The solvent was removed and the oily residue dissolved into the minimum amount of hot EtOH. H $_2$ O was added on cooling and the mixture left to stand overnight. Pale yellow needles were obtained. ^1H NMR (270 MHz, CDCl $_3$) δ 3.00 (d, 2H, *J* 8.0 Hz, CH $_2$ CHOH), 3.6–3.8 (m, 20H, aliphatic crown), 4.79 (t, 1H, *J* 8.0 Hz, CH $_2$ CHOH), 6.62 (d, 2H, *J* 8.1 Hz, Ar), 7.1–7.2 (m, 4H, Ar, pyridyl) 8.40 (d, 2H, *J* 5.4 Hz, pyridyl).

1-[4-(*E*)-2-pyridinyl-4-yl]phenyl]-4,7,10,13-tetraoxa-1-azacyclopentadecane (L1a). This was synthesised from **4** by following a reported procedure for an NEt $_2$ derivative.¹⁷ The alcohol was dissolved into 30 cm 3 of 10% (v/v) aqueous H $_2$ SO $_4$ in a round-bottomed flask and heated to 90 °C for 2 h. The red–orange solution was cooled and neutralised by adding 1 mol dm $^{-3}$ aqueous NaOH, to yield a yellow precipitate. The precipitate was filtered, washed with H $_2$ O, dissolved into CH $_2$ Cl $_2$ and dried over MgSO $_4$. The product was obtained by evaporation of the solvent and recrystallised from CH $_2$ Cl $_2$ by adding MeOH. The product was obtained as an orange solid. Yield (2 steps from **3**) 27%; ^1H NMR (270 MHz, CDCl $_3$) δ 3.5–3.8 (m, 20H, aliphatic crown), 6.64 (d, 2H, *J* 8.1 Hz, Ar), 6.76 (d, 1H, *J* 16.2 Hz, CH=CHAr), 7.21 (d, 1H, *J* 16.2 Hz, CH=CHAr), 7.29 (d, 2H, *J* 5.9 Hz, pyridyl), 7.39 (d, 2H, *J* 8.1 Hz, Ar), 8.48 (d, 2H, *J* 5.9 Hz, pyridyl).

4-(*E*)-2-phenylvinyl]pyridine (L1b). This was prepared in an identical manner to L1a except that benzaldehyde was used as the starting material instead of the azacrown derivative. The product was obtained as a white solid. Yield (2 steps) 25%. ^1H NMR (270 MHz, CDCl $_3$) δ 7.00 (d, 1H, *J* 17.0 Hz, CH=CHAr), 7.2–7.4 (m, 6H, Ar, pyridyl, CH=CHAr), 7.53 (d, 2H, *J* 8.1 Hz, Ar), 8.56 (d, 2H, *J* 5.4 Hz, pyridyl).

1-[4-(2,2-Dibromovinyl)phenyl]4,7,10,13-tetraoxa-1-azacyclopentadecane (5). This was synthesised from **4** by following a reported procedure for a different aldehyde.¹⁸ Zinc (2.84 g, 44 mmol) and CBr $_4$ (14.6 g, 44 mmol) were mixed in anhydrous CH $_2$ Cl $_2$ and stirred at –15 °C. A solution of PPh $_3$ (11.6 g, 44 mmol) in anhydrous CH $_2$ Cl $_2$ was added dropwise. The reaction mixture was stirred for *ca.* 0.5 h at –15 °C and then stirred at room temperature for *ca.* 3 h. **3** (6.5 g, 20 mmol) was added and the reaction mixture (now dark brown) was stirred at room temperature for 2 h. H $_2$ O was added and the organic phase was extracted with CH $_2$ Cl $_2$, washed with H $_2$ O and dried over anhydrous MgSO $_4$. Removal of the solvent yielded a brown solid which was washed with acetone to remove insoluble by-products, and purified by repeated column chromatography (silica, 5% MeOH/CH $_2$ Cl $_2$). The desired product was obtained

as a very pale yellow oil. Yield 2.3 g (24 %). $^1\text{H NMR}$ (270 MHz, CDCl_3) δ 3.5–3.7 (m, aliphatic crown) 6.60 (d, 2H, J 6.8 Hz, Ar), 7.30 (s, 1H, $\text{Br}_2\text{C}=\text{CHAr}$) 7.44 (d, 2H, J 6.8 Hz, Ar).

1-(4-Ethynylphenyl)-4,7,10,13-tetraoxa-1-azacyclopentadecane (6). This was prepared by following a reported procedure for a different alkyne.¹⁹ 2.3 g of **5** (4.9 mmol) was dissolved into 19 cm^3 of anhydrous THF under N_2 , 2 equiv. of BuLi (6.2 cm^3 , 9.85 mmol) in 5 cm^3 THF was added under N_2 at -78°C , and the mixture was stirred for 1 h at -78°C . The mixture was brought to room temperature and stirred for 1 h, and then H_2O was added. The organic phase was extracted with CH_2Cl_2 , dried over anhydrous MgSO_4 and the solvent removed. A yellow oil was obtained. $^1\text{H NMR}$ (270 MHz, CDCl_3) δ 2.93 (s, 1H, $\text{C}\equiv\text{CH}$) 3.5–3.7 (m, aliphatic crown) 6.53 (d, 2H, J 10.8 Hz, Ar), 7.29 (d, 2H, J 10.8 Hz, Ar).

1-(4-(Pyridin-4ylethynyl)phenyl)-4,7,10,13-tetraoxa-1-azacyclopentadecane (L2a). This was prepared by following a reported procedure for a different alkyne.²⁰ **6** (1.4 g, 4.4 mmol), 4-bromopyridine hydrochloride (1.02 g, 5.3 mmol), dichlorobis(triphenylphosphine)palladium(II) (16.8 mg, 0.02 mmol) and copper(I) iodide (6.9 mg, 0.04 mmol) were stirred in 5 ml diethylamine for 3 h at room temperature followed by stirring for 2 h at reflux. After cooling to room temperature, the diethylamine was removed under vacuum on a Schlenk line and then a saturated aqueous NH_4Cl solution was added to the residue. The organic material was extracted with diethyl ether, washed with a solution of NH_4Cl , dried over anhydrous MgSO_4 , and the solvent removed to yield a dark solid. This was purified *via* column chromatography (5% MeOH/ CH_2Cl_2 on silica) to yield the desired product as a pale yellow solid. Yield 856 mg (50 %). $^1\text{H NMR}$ (270 MHz, CDCl_3) δ 3.5–3.7 (m, aliphatic crown) 6.60 (d, 2H, J 9.0 Hz, Ar), 7.30 (d, 2H, J 5.4 Hz, pyridyl) 7.37 (d, 2H, J 9.0 Hz, Ar), 8.52 (d, 2H, J 5.4 Hz, pyridyl).

4-(Phenylethynyl)pyridine (L2b). This was prepared in an identical manner to **L2a** except that ethynylbenzene (1.87 g, 18 mmol) was used as the starting material instead of **6**. The product was obtained as white crystals. Yield 1.7 g (52 %). $^1\text{H NMR}$ (270 MHz, CDCl_3) δ 7.2–7.4 (m, 5H, Ar, pyridyl), 7.53 (m, 2H, Ar), 8.58 (d, 2H, J 5.4 Hz, pyridyl).

Re complexes

The Re complexes were prepared by following a procedure reported for other L ligands;^{13,21} the synthesis of model **1b** has been reported previously.⁴⁷ $(\text{bpy})\text{Re}(\text{CO})_3\text{Cl}$ was prepared by refluxing $\text{Re}(\text{CO})_5\text{Cl}$ with 3 equiv. of 2,2-bipyridyl in toluene for ca. 3 h. $(\text{bpy})\text{Re}(\text{CO})_3\text{Cl}$ was then stirred with an excess of $\text{CF}_3\text{SO}_3\text{H}$ at room temperature for 1 h to yield $(\text{bpy})\text{Re}(\text{CO})_3(\text{CF}_3\text{SO}_3)$, which was refluxed overnight in THF under N_2 with <1 equiv. of the appropriate L ligand. The product was metathesized with NH_4PF_6 to yield $[(\text{bpy})\text{Re}(\text{CO})_3\text{L}]\text{PF}_6$, which was purified by repeated recrystallization and column chromatography (5% MeOH/ CH_2Cl_2 eluting on silica) and characterized by IR, ES-MS, $^1\text{H-NMR}$, and elemental analysis. $^1\text{H NMR}$ showed that the *trans*-isomers of the styryl complexes (**1a** and **1b**) were formed exclusively. Yields were typically 40–50% following chromatography.

$[(\text{bpy})\text{Re}(\text{CO})_3(\text{L1a})]\text{PF}_6$ (1a). The product was obtained as an orange–red solid. $^1\text{H NMR}$ (270 MHz, CDCl_3) δ 3.5–3.7 (m, 20H, aliphatic crown), 6.56 (d, 1H, J 16.7 Hz, $\text{CH}=\text{CHAr}$), 6.59 (d, 2H, J 8.1 Hz, Ar), 7.19 (d, 1H, J 16.7 Hz, $\text{CH}=\text{CHAr}$), 7.21 (d, 2H, J 7.0 Hz, pyridyl), 7.31 (d, 2H, J 8.1 Hz, Ar), 7.70 (t, 2H, J 5.4 Hz, bpy), 7.85 (d, 2H, J 7.0 Hz, pyridyl), 8.25 (t, 2H, J 8.1 Hz, bpy), 8.53 (d, 2H, J 8.1 Hz, bpy), 9.05 (d, 2H, J 5.4 Hz, bpy); ESI MS m/z (relative intensity %) 825 (M^+ ,

$\text{C}_{36}\text{H}_{38}\text{N}_4\text{O}_7\text{Re}$, 100); IR (ν_{CO} , CH_2Cl_2 ; cm^{-1}): 2035, 1931. Anal. Calcd. for $\text{C}_{36}\text{H}_{38}\text{N}_4\text{O}_7\text{RePF}_6$: C, 44.58; H, 3.95; N, 5.78. Found: C, 43.05; H, 3.85; N, 5.62.

$[(\text{bpy})\text{Re}(\text{CO})_3(\text{L1b})]\text{PF}_6$ (1b). The product was obtained as a crystalline yellow solid. $^1\text{H NMR}$ (270 MHz, CDCl_3) δ 6.85 (d, 1H, J 16.7 Hz, $\text{CH}=\text{CHAr}$), 7.03 (d, 2H, J 8.1 Hz, Ar), 7.23 (m, 6H, Ar, pyridyl, $\text{CH}=\text{CHAr}$), 7.66 (t, 2H, J 5.4 Hz, bpy), 8.10 (m, 4H, bpy, pyridyl) 8.39 (d, 2H, J 8.1 Hz, bpy), 9.14 (d, 2H, J 5.4 Hz, bpy); ESI MS m/z (relative intensity %) 608 (M^+ , $\text{C}_{26}\text{H}_{18}\text{N}_3\text{O}_3\text{Re}$, 100); IR (ν_{CO} , CH_2Cl_2 ; cm^{-1}): 2035, 1931.

$[(\text{bpy})\text{Re}(\text{CO})_3(\text{L2a})]\text{PF}_6$ (2a). The product was obtained as a yellow solid. $^1\text{H NMR}$ (270 MHz, CDCl_3) δ 3.5–3.7 (m, 20H, aliphatic crown), 6.54 (d, 2H, J 8.1 Hz, Ar), 7.22 (d, 2H, J 6.5 Hz, pyridyl), 7.29 (d, 2H, J 8.1 Hz, Ar), 7.72 (t, 2H, J 5.4 Hz, bpy) 7.95 (d, 2H, J 6.5 Hz, pyridyl), 8.26 (t, 2H, J 8.1 Hz, bpy), 8.54 (d, 2H, J 8.1 Hz, bpy), 9.05 (d, 2H, J 5.4 Hz, bpy); ESI MS m/z (relative intensity %) 823 (M^+ , $\text{C}_{36}\text{H}_{38}\text{N}_4\text{O}_7\text{Re}$, 100); IR (ν_{CO} , CH_2Cl_2 ; cm^{-1}): 2035, 1931. Anal. Calcd. for $\text{C}_{36}\text{H}_{38}\text{N}_4\text{O}_7\text{RePF}_6$: C, 44.67; H, 3.75; N, 5.79. Found: C, 44.21; H, 3.77; N, 5.68.

$[(\text{bpy})\text{Re}(\text{CO})_3(\text{L2b})]\text{PF}_6$ (2b). The product was obtained as a crystalline yellow solid. $^1\text{H NMR}$ (270 MHz, CDCl_3) δ 7.21 (m, 7H, Ar, pyridyl), 7.72 (t, 2H, J 5.4 Hz, bpy), 8.19 (t, 2H, J 8.1 Hz, bpy), 8.27 (d, 2H, J 6.7 Hz, pyridyl), 8.45 (d, 2H, J 8.1 Hz, bpy), 9.19 (d, 2H, J 5.4 Hz, bpy); ESI MS m/z (relative intensity %) 606 (M^+ , $\text{C}_{26}\text{H}_{16}\text{N}_3\text{O}_3\text{Re}$, 100); IR (ν_{CO} , CH_2Cl_2 ; cm^{-1}): 2036, 1932. Anal. Calcd. for $\text{C}_{26}\text{H}_{17}\text{N}_3\text{O}_3\text{RePF}_6$: C, 41.60; H, 2.28; N, 5.60. Found: C, 41.54; H, 2.34; N, 5.63.

Acknowledgements

We thank Professor Robin Perutz for his assistance and advice, Dr Trevor Dransfield for recording mass spectra, and Ms Heather Fish and Ms Kirsten Ampt for recording NMR spectra. We acknowledge financial support from ESPRC.

References

- A. P. de Silva, H. Q. N. Gunaratne, T. Gunnlaugsson, A. J. M. Huxley, C. P. McCoy, J. T. Rademacher and T. E. Rice, *Chem. Rev.*, 1997, **97**, 1515.
- L. Fabbri and A. Poggi, *Chem. Soc. Rev.*, 1995, 197.
- A. P. de Silva and C. P. McCoy, *Chem. Ind.*, 1994, 992.
- B. Valeur and E. Bardez, *Chem. Br.*, 1995, 216.
- H.-G. Lohr and F. Vögtle, *Acc. Chem. Res.*, 1985, **18**, 65.
- J. Bourson and B. Valeur, *J. Phys. Chem.*, 1989, **93**, 3871.
- I. K. Lednev, R. E. Hester and J. N. Moore, *J. Chem. Soc., Faraday Trans.*, 1997, **93**, 1551.
- I. K. Lednev, R. E. Hester and J. N. Moore, *J. Phys. Chem.*, 1997, **101**, 7371.
- R. M. Mathevet, G. Jonusauskas, C. Rullière, J.-F. Létard and R. Lapouyade, *J. Phys. Chem.*, 1995, **99**, 15709.
- J. D. Lewis, R. N. Perutz and J. N. Moore, *Chem. Commun.*, 2000, 1865.
- J. D. Lewis and J. N. Moore, *Chem. Commun.*, 2003, 2858.
- K. S. Schanze, D. B. MacQueen, T. A. Perkins and L. A. Cabana, *Coord. Chem. Rev.*, 1993, **122**, 63.
- D. B. MacQueen and K. S. Schanze, *J. Am. Chem. Soc.*, 1991, **113**, 6108.
- J. D. Lewis, R. N. Perutz and J. N. Moore, *J. Phys. Chem. A*, 2002, **106**, 12202.
- M. V. Alfimov, A. V. Churakov, Y. V. Fedorov, O. A. Fedorova, S. P. Gromov, R. E. Hester, J. A. K. Howard, L. G. Kuz'mina, I. K. Lednev and J. N. Moore, *J. Chem. Soc., Perkin Trans. 2*, 1997, 2249.
- J. P. Dix and F. Vögtle, *Chem. Ber.*, 1980, **113**, 457.
- A. Juris, S. Campagna, I. Bidd, J.-M. Lehn and R. Ziessel, *Inorg. Chem.*, 1988, **27**, 4007.
- A. de Meijere, S. Kozhushkov, T. Haumann, R. Boese, C. Puls, M. J. Cooney and L. T. Scott, *Chem. Eur. J.*, 1995, **1**, 124.
- E. J. Corey and P. L. Fuchs, *Tetrahedron Lett.*, 1972, 3769.

- 20 J. Okubo, H. Shinozaki, T. Koitabashi and R. Yomura, *Bull. Chem. Soc. Jpn.*, 1998, **71**, 329.
- 21 B. B. Sullivan and T. J. Meyer, *Chem. Commun.*, 1984, 1244.
- 22 K. Kalyandasundaram, *J. Chem. Soc., Faraday Trans.*, 1986, **82**, 2401.
- 23 C. J. Pouchert and J. Behnke, *Aldrich Library of ^{13}C and ^1H FT NMR spectra*, Aldrich Chemical Company Inc., Milwaukee, WI, 1st edn., 1993.
- 24 R. D. Shannon, *Acta Crystallogr.*, 1976, **A32**, 751.
- 25 B. Brzezinski, G. Schroeder, A. Rabold and G. Zundel, *J. Phys. Chem.*, 1995, **99**, 8519.
- 26 Alternative plots of the shift in peak absorbance in wavenumbers (cm^{-1}) versus the ionic index z^2/r (\AA^{-1}) do not give a linear plot,²⁷ although there is a broad correlation which is more linear than that shown in Fig. 5.
- 27 K. Rurack, J. L. Bricks, G. Reck, R. Radeaglia and U. Resch-Genger, *J. Phys. Chem. A*, 2000, **104**, 3087.
- 28 Our time-resolved studies of the photochemical release and thermal binding of Li^+ to Re-azacrown complexes also support this interpretation; they will be reported elsewhere.
- 29 Addition of excess HCl or HClO_4 to an NMR sample of **2a** (ca. 1×10^{-3} mol dm^{-3}) resulted in a complicated ^1H NMR spectrum which was quite different from the others reported here and may indicate that a reaction occurred at these high concentrations; this effect was not studied further.
- 30 The purpose of these measurements was to determine the positions of the resonances from **1a**- M^{n+} and **2a**- M^{n+} , and so samples of fully complexed species were studied; samples comprising both metal-free and metal-complexed forms may show single resonances with positions dependent on the sample composition because the literature indicates that exchange would be fast on the NMR time scale.³¹
- 31 (a) F. Hallwass, M. Engelsberg, A. M. Simas and W. Barros, *Chem. Phys. Lett.*, 2001, **335**, 43; (b) K. M. Brière and C. Detellier, *Can. J. Chem.*, 1992, **70**, 2536; (c) P. Szczygiel, M. Shamsipur, K. Hallenga and A. I. Popov, *J. Phys. Chem.*, 1987, **91**, 1252.
- 32 J. Bourson, J. Pouget and B. Valeur, *J. Phys. Chem.*, 1993, **97**, 4552.
- 33 S. Fery-Forgues, M.-T. LeBris, J.-P. Guetté and B. Valeur, *J. Phys. Chem.*, 1988, **92**, 6233.
- 34 J. F. Létard, R. Lapouyade and W. Rettig, *Pure Appl. Chem.*, 1993, **65**, 1705.
- 35 R. M. Izatt, K. Pawlak, J. S. Bradshaw and R. L. Bruening, *Chem. Rev.*, 1991, **91**, 1721.
- 36 K. Rurack, M. Sczepan, M. Spieles, U. Resch-Genger and W. Rettig, *Chem. Phys. Lett.*, 2000, **320**, 87.
- 37 J.-F. Létard, S. Delmond, R. Lapouyade, D. Braun, W. Rettig and M. Kriessler, *Recl. Trav. Chim. Pays-Bas.*, 1995, **114**, 517.
- 38 L. Antonov, M. Vladimirova, E. Stanoeva, W. M. F. Fabian, L. Ballester and M. Mitewa, *J. Inclusion Phenom. Macrocycl. Chem.*, 2001, **40**, 23.
- 39 Plots of $\log K$ versus the ionic index z^2/r (\AA^{-1}) do not give a linear plot,²⁷ although there is a broad correlation.
- 40 R. M. Izatt, K. Pawlak, J. S. Bradshaw and R. L. Bruening, *Chem. Rev.*, 1995, **95**, 2529.
- 41 M. J. G. Lesley, A. Woodward, N. J. Taylor, T. B. Marder, I. Cazenobe, I. Ledoux, J. Zyss, A. Thornton, D. W. Bruce and A. K. Kakkar, *Chem. Mater.*, 1998, **10**, 1355.
- 42 D. Roberto, R. Ugo, S. Bruni, E. Cariati, F. Cariati, P. Fantucci, I. Invernizzi, S. Quici, I. Ledoux and J. Zyss, *Organometallics*, 2000, **19**, 1775.
- 43 L. De Cola and P. Belser, *Coord. Chem. Rev.*, 1998, **177**, 301.
- 44 L.-T. Cheng, W. Tam, S. R. Marder, A. E. Stiegman, G. Rikken and C. W. Spangler, *J. Phys. Chem.*, 1991, **95**, 10643.
- 45 T. E. O. Screen, I. M. Blake, L. H. Rees, W. Clegg, S. J. Borwick and H. L. Anderson, *J. Chem. Soc., Perkin Trans. 1*, 2002, 320.
- 46 Gaussian 98, Revision A.7, M. J. Frisch, G. W. Trucks, H. B. Schlegel, G. E. Scuseria, M. A. Robb, J. R. Cheeseman, V. G. Zakrzewski, J. A. Montgomery, Jr., R. E. Stratmann, J. C. Burant, S. Dapprich, J. M. Millam, A. D. Daniels, K. N. Kudin, M. C. Strain, O. Farkas, J. Tomasi, V. Barone, M. Cossi, R. Cammi, B. Mennucci, C. Pomelli, C. Adamo, S. Clifford, J. Ochterski, G. A. Petersson, P. Y. Ayala, Q. Cui, K. Morokuma, D. K. Malick, A. D. Rabuck, K. Raghavachari, J. B. Foresman, J. Cioslowski, J. V. Ortiz, A. G. Baboul, B. B. Stefanov, G. Liu, A. Liashenko, P. Piskorz, I. Komaromi, R. Gomperts, R. L. Martin, D. J. Fox, T. Keith, M. A. Al-Laham, C. Y. Peng, A. Nanayakkara, C. Gonzalez, M. Challacombe, P. M. W. Gill, B. Johnson, W. Chen, M. W. Wong, J. L. Andres, C. Gonzalez, M. Head-Gordon, E. S. Replogle and J. A. Pople, Gaussian, Inc., Pittsburgh PA, 1998.
- 47 V. W.-W. Yam, V. C.-Y. Lau and L.-X. Wu, *J. Chem. Soc., Dalton Trans.*, 1998, 1461.